Variable-Energy Photoelectron Spectroscopy of $CpM(CO)_2$ (M = Co, Rh, Ir): Molecular Orbital Assignments and an Evaluation of the Difference in Ground-State Orbital Characters

Xiaorong Li, G. Michael Bancroft,* Richard J. Puddephatt,* Yong-Feng Hu, and Kim H. Tan

Department of Chemistry, University of Western Ontario, London, Ontario, Canada N6A 5B7, and Canadian Synchrotron Radiation Facility, Synchrotron Radiation Centre, University of Wisconsin−Madison, Stoughton, Wisconsin 53589

Received March 19, 1996[⊗]

Photoelectron (PE) spectra with variable photon energy have been recorded between 21 and 70 eV using He I, He II, and synchrotron radiation for the cobalt, rhodium, and iridium complexes $CpM(CO)_2$, where Cp is η^5-cyclopentadienyl. The spectra have been assigned on the basis of Xα-SW molecular orbital (MO) calculations for the ground-state $CpM(CO)_2$ molecules and by consideration of trends in photoelectron band intensities as a function of the energy of the radiation used. Photoionization cross sections (σ) have been calculated for the valence ionizations of the three molecules, using both the Xα-SW and Gelius methods. The theoretical branching ratios ($\sigma_i/\sum\sigma$) from both theoretical methods have been compared with the observed branching ratios ($A_i/\sum A$) between 21 and 70 eV. Our assignment (from the He I and He II spectra and the agreement between theoretical and observed branching ratios between 21 and 70 eV) gives a similar ordering of ionization potentials (IP's) for $CpCo(CO)_2$ and $CpRh(CO)_2$ with those reported in the literature. However, both the variable-energy valence photoelectron spectra and the Xα-SW calculations indicate a greater difference than was proposed previously in ground-state orbital composition between the HOMO's of these two compounds. The assignment of PE spectra of the newly recorded molecule $CpIr(CO)_2$ is the same as that for the Rh analogue. The vibrational structures of the first two ionization bands of $CpIr(CO)_2$ are also observed. The linear regressions of experimental branching ratios versus photon energy plots for HOMO orbitals show strikingly different slopes between Co and Rh or Ir spectra (Co, 0.0542; Rh, −0.175; Ir, −0.114), providing direct evidence for a large difference in ion state orbital characters, which correlate with the ground-state d energy difference descending the transition metal group. IP sequences are compared with the ground-state MO orderings calculated by the Xα-SW method. The changes in the valence ionizations from cobalt to rhodium and iridium are well correlated with the energy separations in the ground state rather than those in the ion state. Hence, reorganization effects do not appear to dominate the trend in the IP's. The complete inner valence spectra of all three complexes have also been assigned with the aid of the Xα-SW energy calculations. The σ MO's having 5σ CO and metal d characters have been assigned in this region for the three compounds at 14.4 eV (Co), 15.2 eV (Rh), and 15.4 eV (Ir), respectively. The apparent shift of this band energy from the first-row to the second- or third-row transition-metal carbonyl is consistent with the shift in outer valence IP's.

Introduction

For many fundamentally important organometallic molecules such as $M(CO)_6$ (M = Cr, Mo, W),[1] $M(\eta^5\text{-}C_5H_5)_2$ (M = Fe, Rh, Os),[2] and $M(\eta^3\text{-}C_3H_5)_2$ (M = Ni, Pd, and Pt),[3a] the molecular orbital (MO) ordering assigned from photoelectron (PE) spectra and MO calculations is on a sound footing. Two factors are important for these confident assignments. First, the MO assignments were all verified by variable-energy photoelectron spectroscopy using synchrotron radiation; second, the studies were undertaken for an entire transition-metal group. In this work, we investigate another series of organometallic compounds, $CpM(CO)_2$ (M = Co, Rh, Ir), by using the variable photon energy technique and Xα-SW calculations.

For organometallic compounds of the cobalt group, the traditional He I and He II photoelectron spectroscopic studies have been reported for several compounds, including CpM(diene) (M = Co, Rh, Ir),[4a] $CpM(CO)_2$ (M

* To whom correspondence should be addressed at the University of Western Ontario.

[⊗] Abstract published in *Advance ACS Abstracts,* June 1, 1996.

(1) Cooper, G.; Green, J. C.; Payne, M. P.; Dobson, B. R.; Hillier, I. H. *J. Am. Chem. Soc.* **1987**, *109*, 3836.

(2) Cooper, G.; Green, J. C.; Payne, M. P. *Mol. Phys.* **1988**, *63*, 1031.

(3) (a) Li, X.; Bancroft, G. M.; Puddephatt, R. J.; Liu, Z. F.; Hu, Y. F.; Tan, K. H. *J. Am. Chem. Soc.* **1994**, *116*, 9543. (b) Li, X.; Tse, J. S.; Bancroft, G. M.; Puddephatt, R. J.; Tan, K. H. *Organometallics* **1995**, *14*, 4513. (c) Li, X.; Bancroft, G. M.; Puddephatt, R. J.; Yuan, Z.; Tan, K. H. *Inorg. Chem.*, submitted for publication. (d) Li, X.; Tse, J. S.; Bancroft, G. M.; Puddephatt, R. J.; Tan, K. H. *Inorg. Chem.*, in press.

(4) (a) Green, J. C.; Powell, P.; van Tilborg, J. E. *Organometallics* **1984**, *3*, 211. (b) Lichtenberger, D. L.; Calabro, D. C.; Kellogg, G. E. *Organometallics* **1984**, *3*, 1623. (c) Pudeney, N.; Kirchner, O. N.; Green, J. C.; Maitlis, P. M. *J. Chem. Soc., Dalton Trans.* **1984**, 1877.

S0276-7333(96)00202-6 CCC: $12.00

= Co and Rh),[4b] and $Cp^*M(CO)_2$ (M = Co, Rh, Ir; Cp^* = $(CH_3)_5Cp$). The ionization trends and intensity changes from He I to He II photon energies along with an MO scheme derived either from qualitative arguments or from Fenske−Hall calculations have been used in these papers to make the assignments. The assignments of the valence ionizations are not trivial, and there is still some uncertainty. In the first study,[4a] the bands with the lowest ionization potential (IP) in the spectra of cobalt complexes have the characteristics of an ionization from an orbital having significant metal d character. In contrast, in the rhodium and iridium complexes, the lowest ionization potential bands have all the characteristics of ionization from a largely ligand-based orbital with rather low metal d character. The valence ionization difference between cobalt and rhodium or iridium spectra was attributed to the different MO compositions of HOMO's between those molecules, which is a ground-state effect. However, in the second study,[4b] it was pointed out that the changes in ground-state electron distributions are not primarily responsible for the shifts in the valence ionizations between these cobalt and rhodium complexes; the greater electron relaxation energy associated with cobalt 3d ionizations is a major factor for their lower ionization energies in comparison to the rhodium complexes.

In this paper, our major objective was to seek the cause of the valence ionization difference between the first-row and the second- or third-row late-transition-metal compounds by investigating (1) the difference in the trends of experimental branching ratios for the HOMO's of the three compounds and (2) the orderings of IP and ground-state Xα eigenvalues. The study of band intensity variation with tunable synchrotron radiation is a good way to correlate the d orbital characters from the ion state measurements with that expected from the ground state MO calculations.[3,5] The spectrum of $CpIr(CO)_2$ has not been reported before. To our knowledge, no MO compositional comparison has been done between the title compounds. No Xα calculation has been reported for $CpRh(CO)_2$, and no calculations of any kind have been published for $CpIr(CO)_2$.

In the past, high-resolution inner valence photoelectron spectra of organometallic compounds have never been obtained due to severe band overlap in this region and to the limit of binding energy range probed by laboratory UV light sources. The other possible reason for ignoring this spectral region is that the inner valence always belongs to the pure ligand MO's in some compounds, and not much information can be obtained in this region on bonding between ligand and metal d orbitals, such as the case for $M(\eta^3\text{-}C_3H_5)_2$ (M = Ni, Pd, Pt).[3a] In studying the PE spectra of $CpM(CO)_2$ (M = Co, Rh, Ir), we could not overlook the inner valence region since MO's such as the σ bonds between metal d and 5σ CO are located there. The relative strength of these bonds in the series can provide us with important information about bonding. With the advent of synchrotron radiation sources, it has become possible to obtain high-quality inner valence band photoelectron spectra.[6] In this paper, we have also carried out studies for the inner valence photoelectron spectra of the title compounds.

Experimental Section

$CpRh(CO)_2$ was synthesized by methods in the literature.[7] $CpIr(CO)_2$ was prepared by using the same method, except that the starting material is $Ir(CO)_3Cl$ (purchased from Strem Chemicals, Inc.). $CpCo(CO)_2$ (technical grade) was purchased from Aldrich and chromatographed under a nitrogen atmosphere in petroleum ether on alumina (neutral, Brockmann grade III, deoxygenized under vacuum and at high temperature before using). Samples were purified by vacuum sublimation, and purity was established by NMR. Samples were stored at −78 °C under an inert atmosphere.

All samples were introduced into the gas cell of two different photoelectron spectrometers by sublimation. The He I and He II spectra of the compounds were obtained using an ESCA 36 spectrometer with a resolution of ∼20 meV.[8] The variable-energy spectra from 20 to 70 eV were obtained at the Canadian Synchrotron Radiation Facility (CSRF) at the Aladdin storage ring using a modified ESCA 36 spectrometer fitted with a Quantar #36 position sensitive detector.[9,10] The Grasshopper grazing incidence monochromator has been described previously.[11] Briefly, photoelectrons were collected at the pseudo magic angle calculated assuming 90% polarization of the synchrotron light. This ensures that the photoelectron intensities obtained are independent of well-known angular effects. Differential pumping of the gas cell maintains a pressure differential of better than 10^4 between the gas cell and the energy analyzer. A light pipe separating the gas cell from the Grasshopper monochromator further ensures long-term stability of the system. Broad-scan and narrow-scan spectra of both valence and inner valence regions were recorded between 20 and 70 eV photon energy at a resolution of *ca.* 100 meV. The He I spectrum was calibrated with the Ar $3p_{3/2}$ line at 15.759 eV. For the synchrotron radiation spectra, the Xe 5s main line at 23.397 eV was used as the calibrant.

For the cross-section analyses, many of the spectra were fit to Gaussian−Lorentzian line shapes using an iterative procedure.[12] Band positions, widths, and shapes were normally constrained to obtain consistent fits from one photon energy to another. Correction of the areas for the electron analyzer transmission was performed by dividing the computed area by the kinetic energy of the band. Experimental branching ratios (BR) were obtained using the resulting band areas (A_i) and the branching ratio formula $BR_i = A_i/\sum A$.

Computational Details

Orbital energies and compositions of $CpM(CO)_2$, $M(CO)_2$, and Cp were calculated using the Xα-SW method as described earlier.[13] Although the Xα method is not the state-of-the-art method today for obtaining MO energies, it has been found to give reliable energies on very large molecules, including very large, low-symmetry, low-space-filling organometallic molecules.[3,5] More importantly, it is the only readily accepted method for obtaining cross sections, and it has consistently given reliable trends in cross sections. The geometry for $CpCo(CO)_2$ was taken from the crystal structure of $Cp^*Co(CO)_2$,[14a] which has the same local structure as $CpCo(CO)_2$.[14b] Since no structural information is available for $CpRh(CO)_2$ and $CpIr(CO)_2$, we used the same crystal parameters for the Rh and Ir compounds as for the Co compound except that the atomic radii of Rh and Ir are increased from 1.67 Å (Co) to 1.83 Å (Rh) and

(5) Green, J. C.; Kaltsoyannis, N.; Sze, K. H.; MacDonald, M. *J. Am. Chem. Soc.* **1994**, *116*, 1994.
(6) Hu, Y. F.; Bancroft, G. M.; Liu, Z. F.; Tan, K. H. *Inorg. Chem.* **1995**, *34*, 3716.
(7) Dickson, R. S.; Tailby, G. R. *Aust. J. Chem.* **1970**, *23*, 1531.
(8) Bancroft, G. M.; Bristow, D. J.; Coatsworth, L. L. *Chem. Phys. Lett.* **1981**, *82*, 344.
(9) Bozek, J. D.; Cutler, J. N.; Bancroft, G. M.; Coatsworth, L. L.; Tan, K. H.; Yang, D. S. *Chem. Phys. Lett.* **1990**, *165*, 1.
(10) Liu, Z. F.; Coatsworth, L. L.; Tan, K. H. *Chem. Phys. Lett.* **1993**, *203*, 337.
(11) (a) Tan, K. H.; Bancroft, G. M.; Coatsworth, L. L.; Yates, B. W. *Can. J. Phys.* **1982**, *60*, 131. (b) Bancroft, G. M.; Bozek, J. D.; Tan, K. H. *Phys. Can.* **1987**, 113.
(12) Bancroft, G. M.; Adams, J.; Coatsworth, L. L.; Bennewitx, C. D.; Brown, J. D.; Westwood, W. D. *Anal. Chem.* **1975**, *47*, 586.

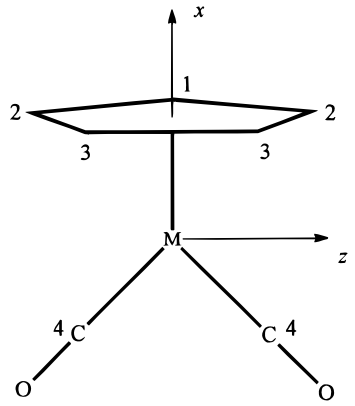

Figure 1. Structure of $CpM(CO)_2$ (M = Co, Rh, Ir; numbers represent the identical groups of carbon atoms in C_s symmetry, see Table 2).

1.87 Å (Ir), respectively.[15] This difference in atomic radii is consistent with the difference in bond lengths between Cp*Co-$(CO)_2$[4a] and Cp*Rh$(CO)_2$.[20] The structures of these last two compounds are essentially identical.[4c] C_s symmetry was assumed for all species. For $CpM(CO)_2$ structures, the *z* axis was taken according to normal conventions as being perpendicular to the mirror plane of the molecule, with the metal atom located at the origin (Figure 1). The exchange α parameters used in each atomic region were taken from Schwarz's tabulation,[16] except for hydrogen, for which 0.777 25 was used. Overlapping atomic sphere radii were used with the outer-sphere radius tangent to the outermost atomic spheres. An l_{max} value of 4 was used around the outer-sphere region, whereas l_{max} values of 3, 1, and 0 were used around M (M = Co, Rh, Ir), C, and H atoms, respectively. Geometries and coordinates of $M(CO)_2$ and Cp are the same as those in CpM-$(CO)_2$. In order to better correlate the orbitals of $M(CO)_2$ with Cp fragments, C_s symmetries are still assumed for the $M(CO)_2$ fragments. Photoionization cross-sections were calculated for the outer valence levels of $CpM(CO)_2$ using the Xα-SW cross section program of Davenport.[17] The calculations were performed with the converged Xα-SW HOMO transition-state potential, modified with a Latter tail to correct for large *r* behavior. In addition to the parameters used in the Xα-SW calculations on molecular orbitals, the maximum azimuthal quantum number, l_{max}, for final states was extended to 8, 4, 3, and 1 around the outer sphere, metal, carbon, and hydrogen region, respectively. In calculations of transition states, half of an electron is removed from the HOMO's of molecular orbitals. All symmetry-allowed photoionization processes based on the dipolar selection rule were included in the calculations.

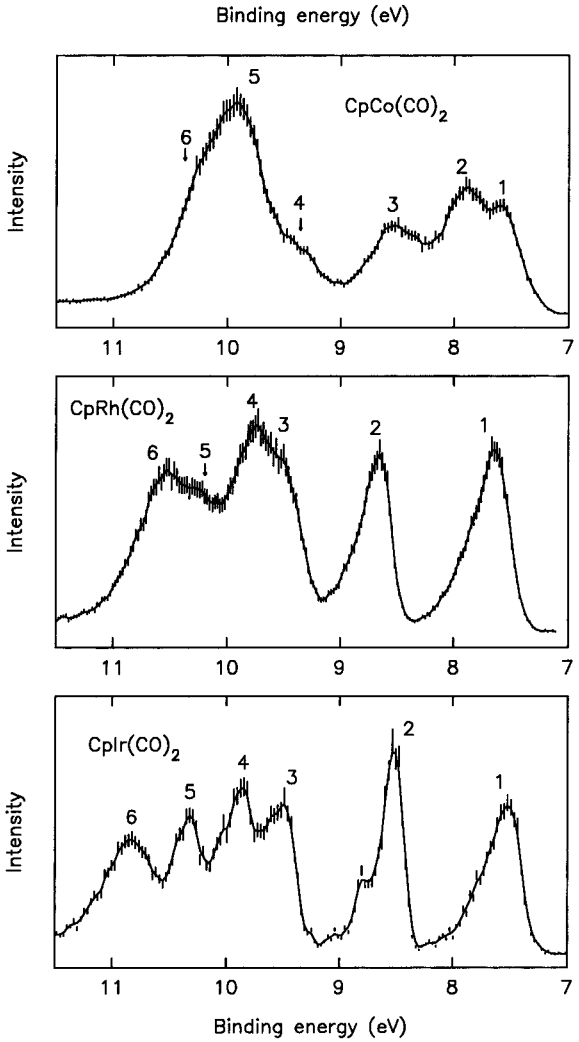

Figure 2. He I valence photoelectron spectra (bands 1−6) of the three $CpM(CO)_2$ (M = Co, Rh, Ir) complexes. The solid line links the smoothed data.

Results

(a) Photoelectron Spectra. The He I spectra of the outer valence region for the three compounds are shown in Figure 2. The spectra of the Co and Rh compounds are identical with the spectra reported previously,[4b] and the spectra of all three compounds are very similar to those for the three Cp* analogues, with a chemical shift of most bands of 0.6 ± 0.2 eV for the Cp* analogues.[4c] The spectrum of the Ir compound is very similar to the Rh spectrum, and it is apparent that the Ir and Rh spectra are qualitatively different from the Co spectrum. This same general effect was seen for the $M(\eta^3\text{-}C_3H_5)_2$ series (M = Ni, Pd, Pt), in which the Ni compound gives a spectrum qualitatively different from those of the Pd and Pt analogues.[3a] In an attempt to resolve more features in the spectra, we recorded narrow-scan spectra of the Rh and Ir complexes. Vibrational structure was evident in bands 1 and 2 of these compounds, with vibrational frequencies of 1790 and 1570 cm^{-1} for the Ir and Rh compounds, respectively.

$CpCo(CO)_2$. The He I spectra and the representative variable-energy spectra of $CpCo(CO)_2$ in the outer valence region are shown in Figures 2 and 3. Bands 1−4 in the low-binding-energy region are resolved. Bands 5 and 6 overlap strongly; therefore, we fit these bands to only one band (Figure 3). Thus there are a

(13) (a) Yang, D. S.; Bancroft, G. M.; Puddephatt, R. J.; Bozek, J. D.; Tse, J. S. *Inorg. Chem.* **1989**, *28*, 1. (b) Yang, D. S.; Bancroft, G. M.; Puddephatt, R. J.; Bursten, B. E.; McKee, S. D. *Inorg. Chem.* **1989**, *28*, 872. (c) Yang, D. S.; Bancroft, G. M.; Puddephatt, R. J. *Inorg. Chem.* **1990**, *29*, 2118. (d) Yang, D. S.; Bancroft, G. M.; Dignard-Bailey, L.; Puddephatt, R. J.; Tse, J. S. *Inorg. Chem.* **1990**, *29*, 2487. (e) Yang, D. S.; Bancroft, G. M.; Puddephatt, R. J.; Tse, J. S. *Inorg. Chem.* **1990**, *29*, 2496. (f) Yang, D. S.; Bancroft, G. M.; Puddephatt, R. J.; Tan, K. H.; Cutler, J. N.; Bozek, J. B. *Inorg. Chem.* **1990**, *29*, 4956. (g) Bursten, B. E.; Casarin, M.; DiBella, S.; Fang, A.; Fragala, I. L. *Inorg. Chem.* **1985**, *24*, 2169. (h) Cotton, F. A.; Stanley, G. G.; Cowley, A. H.; Lattman, M. *Organometallics* **1988**, *7*, 835. (i) Guimon, G.; Pfister-Guillozo, G.; Chaudret, B.; Poiblanc, R. *J. Chem. Soc., Dalton Trans.* **1985**, 43. (j) Bridgeman, A. J.; Davis, L.; Dixon, S. J.; Green, J. C.; Wright, I. N. *J. Chem. Soc., Dalton Trans.* **1995**, 1023.

(14) (a) Byers, L. R.; Dahl, L. F. *Inorg. Chem.* **1980**, *19*, 277. (b) Antipin, M. Y.; Struchkov, Y. T.; Chernega, A. N.; Meidine, M. F.; Nixon, J. F. *J. Organomet. Chem.* **1992**, *436*, 79.

(15) *Table of Periodic Properties of the Elements*; Sargent-Welch Scientific: Skokie, IL, 1980.

(16) (a) Schwarz, K. *Phys. Rev. B* **1972**, *5*, 2466. (b) Schwarz, K. *Theor. Chim. Acta (Berlin)* **1974**, *34*, 225.

(17) (a) Davenport, J. W. Ph.D. Dissertation, University of Pennsylvania, 1976. (b) Davenport, J. W. *Phys. Rev. Lett.* **1976**, *36*, 945.

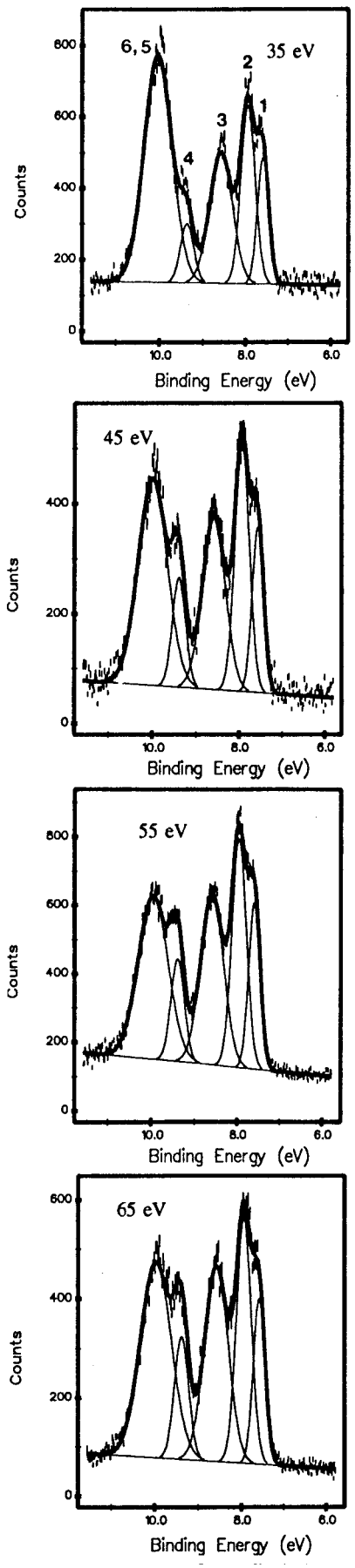

Figure 3. Representative valence photoelectron spectra (bands 1−6) of $CpCo(CO)_2$ at 35, 45, 55, and 65 eV.

total of six bands in the outer valence region corresponding to the six MO's expected from theoretical calculations (four metal-based and two ligand-based MO's).[4b] When the photon energy increases from 21 to 70 eV, the relative variation of band intensity shows that bands 1−4 experience a steady increase in intensity, indicating the high cobalt 3d character associated with them. On the other hand, the intensity of the band which contains bands 5 and 6 decreases, showing a large ligand C 2p character. In particular, the relative intensities vary smoothly over this whole energy range and no metal 3p resonance effect was observed, as will be demonstrated later by the trends in branching ratios. Of greater importance, band 1, which was not resolved in the reported He II spectrum in the literature,[4b] was clearly resolved over this photon energy range. In comparison with bands 2−4, the intensity of band 1 does not change greatly. However, there is a distinct intensity increase compared to the band which contains bands 5 and 6, indicating its large metal 3d character.

The broad-range PE spectrum at 60 eV photon energy, which covers both the outer valence and inner valence regions of $CpCo(CO)_2$ has also been recorded (Figure 4). Another band in the outer valence region, band 7 (13.00 eV), is shown in this spectrum. The comparison between the broad-range spectrum at 60 eV with that at He I photon energy (Figure 1 in ref 4b) shows that the intensity of band 7 decreases greatly from He I energy to 60 eV, indicating its ligand character. In this work, all bands (A−I) with binding energies higher than that for band 7 are arbitrarily defined as being in the inner valence region. As will be seen later, the two overlapped bands (A and B) at 14.40 eV are resolved in the Rh and Ir spectra. The shapes and positions of bands C−I, which are similar to those in PE spectra of $CpM(CO)_3$ (M = Mn, Re),[18] show two adjacent bands (C and D) with relatively narrow width and higher intensity at 17.64 and 18.36 eV, two broad bands (E and F) with medium intensity at 20.03 and 22.77 eV, and three very broad bands (G−I) with low intensity at 26.3, 29.9, and 35.0 eV, respectively.

$CpRh(CO)_2$. The He I and He II spectra and the representative variable-energy spectra of $CpRh(CO)_2$ in the outer valence region are shown in Figures 2, 5, and 6. The spectra demonstrate that the relative intensity of the first band changes in a different way for $CpRh(CO)_2$ than for its Co congener: this band *decreases* in relative intensity from 21 to 70 eV, while for Co, the relative intensity of the first band *increases*. This evidence, which has not been reported before, suggests that the orbital character of the first band in $CpRh(CO)_2$ is qualitatively different from that of $CpCo(CO)_2$. For the Rh compound, the spectra also show that the first band decreases in intensity from 21 to 70 eV, while bands 2, 3, 5, and 6 increase in intensity and band 4 decreases in intensity. These trends are different from those in the spectra of $CpCo(CO)_2$, in which the intensities of the bands at higher binding energies (bands 5 and 6) decrease dramatically from low to high photon energy.

Since bands 4 and 6 in Figure 6 are less resolved, we recorded narrow-scan He I and He II spectra (Figure 5) of the Rh compound to verify the intensity features. Figure 5 shows that the relative intensity of band 4 decreases markedly from He I to He II photon energy, suggesting that it is related to a ligand-based MO, and

(18) Hu, Y. F.; Bancroft, G. M.; Tse, J. S.; Tan, K. H. *Can. J. Chem.*, submitted for publication.

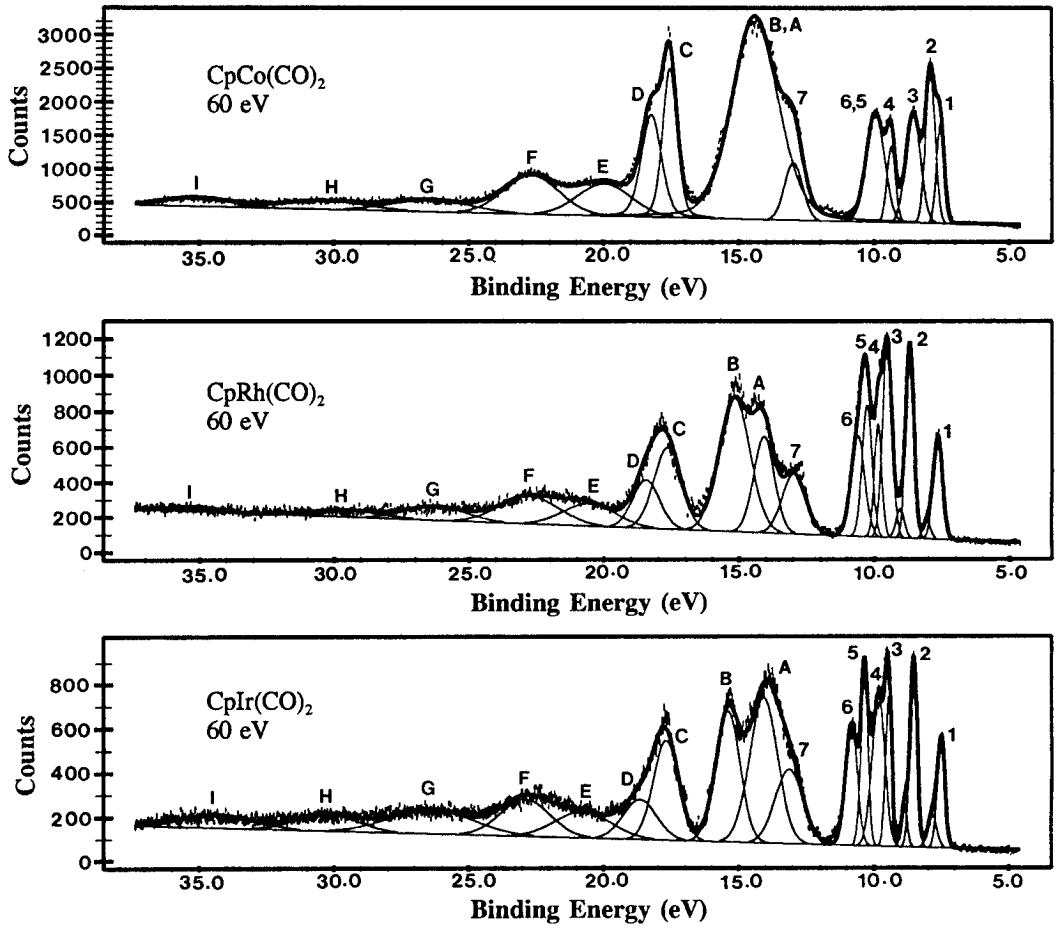

Figure 4. Broad-range PE spectra of $CpM(CO)_2$ (M = Co, Rh, Ir) at 60 eV respectively, showing the outer valence shell (bands 1−7) and inner valence shell (bands A−I) among these three compounds.

bands 3 and 5 are associated with the ionizations of two MO's with large metal 4d character. For band 6, the intensity variation shows that it is from the ionization of a MO with intermediate metal 4d character.

The broad-range PE spectrum at 60 eV, which covers both outer valence (bands 1−7) and inner valence (bands A−I) of $CpRh(CO)_2$, is shown in Figure 4. The comparison between this spectrum and the broad-range He I spectrum (Figure 2 in ref 4b) shows that the intensity of band 7 (12.94 eV) decreases greatly from He I photon energy to 60 eV, indicating its ligand character. Band B (15.2 eV), which overlaps with band A in the Co spectrum, shifts to slightly high binding energy and thus is separated from band A in the Rh spectrum. The increase in intensity from He I energy (Figure 2 in ref 4b) to 60 eV tells us that band B is associated with the ionization from a MO with considerable metal 4d character.

$CpIr(CO)_2$. The He I spectrum and the representative variable-energy spectra of $CpIr(CO)_2$ in the outer valence region are shown in Figures 2 and 7, respectively. The number and distribution of bands between the Rh and Ir spectra are similar, except that the bands are much better resolved in the Ir than in the Rh spectra. However, the spectra of both Rh and Ir complexes differs from those of the Co complex in band shapes and positions. The trends in band intensities are similar for M = Rh, Ir, but both are different from the trend for M = Co. Thus, the relative intensity of the first band decreases from 21 to 70 eV, and the intensities of bands 2, 3, and 5 increase over this energy range, as for the Rh complex. When the He I spectrum

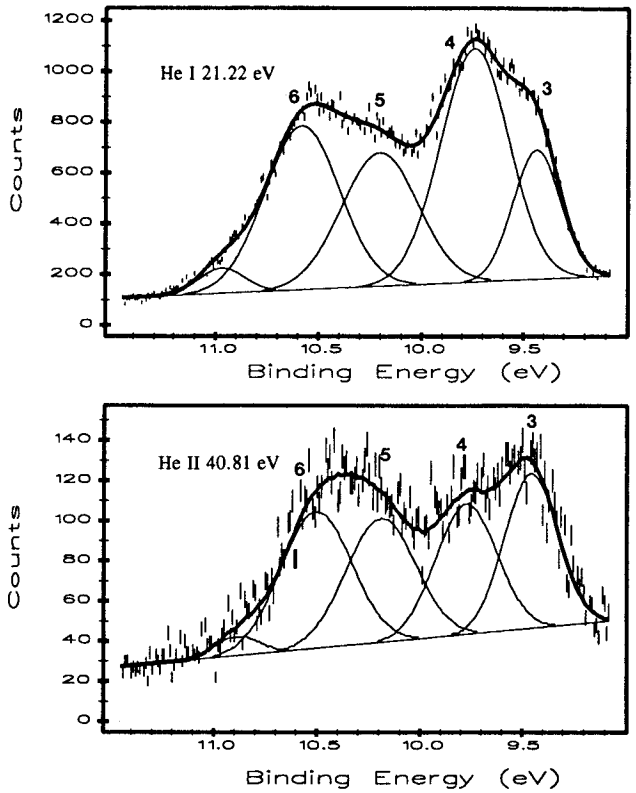

Figure 5. He I and He II spectra of $CpRh(CO)_2$ showing bands 3−6.

of $CpIr(CO)_2$ in Figure 2 is compared with those at high photon energies in Figure 7, it is apparent that bands 4 and 6 decrease in relative intensity. These features

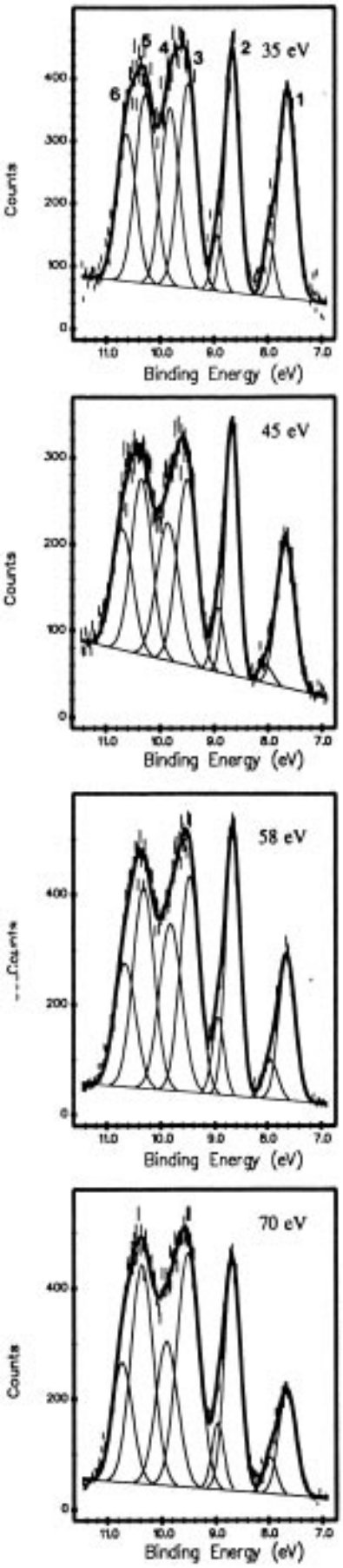

Figure 6. Representative valence photoelectron spectra (bands 1−6) of $CpRh(CO)_2$ at 35, 45, 58, and 70 eV.

indicate that the MO assignments are likely the same for the Rh and Ir complexes.

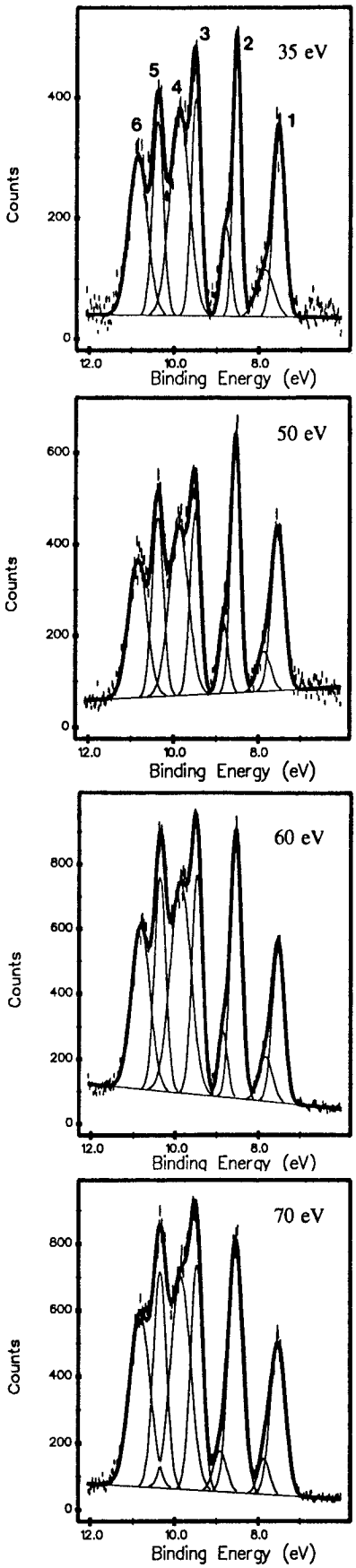

Figure 7. Representative valence photoelectron spectra (bands 1−6) of $CpIr(CO)_2$ at 35, 50, 60, and 70 eV.

The broad-range spectrum of $CpIr(CO)_2$ in the region above 11 eV (bands 7 and A−I) binding energy is similar to that of $CpRh(CO)_2$ (Figure 4), except that band 7 for the Ir complex appears as a shoulder adjacent to band

Table 1. Xα-SW MO Compositions and PES Band Assignments for $CpM(CO)_2$

orbital M = Co	Xα energy (eV)	vertical IP (eV)	band assignt	% 3d Co	% 2p C1	% 2p C2	% 2p C3	% 2p C4	% 2p O
16a′	−5.13	7.59	1	24.9	16.8	4.4	26.3	8.4	12.1
15a′	−6.39	7.94	2	91.6		2.3	0.9	0.6	0.4
11a″	−6.42	10.00	5	31.8	0.2	40.1	14.2	2.3	2.3
14a′	−6.90	8.54	3	84.4	0.1	0.6	0.4	3.6	9.8
10a″	−6.91	9.35	4	90.9	0.5	2.0	0.3	1.7	4.5
13a′	−7.37	10.49	6	69.2	8.9	3.4	14.6	0.6	2.1
12a′	−9.12	13.00	7	4.4	17.9	33.2	33.3		

15a′, 0.6% 2s (C4), 2.4% 4s (Co); 11a″, 2.1% 2s (C4); 12a′, 4.7% 4p (Co), 3.2% 4s (Co)

orbital M = Rh	Xα energy (eV)	vertical IP(eV)	band assignt	% 4d Rh	% 2p C1	% 2p C2	% 2p C3	% 2p C4	% 2p O
16a′	−5.10	7.60	1	16.0	21.5	5.8	33.6	7.6	9.7
11a″	−6.58	9.82	4	23.9	0.2	42.7	14.2	4.3	1.9
15a′	−7.29	8.65	2	84.0		2.7	1.2	2.4	1.1
14a′	−7.89	9.48	3	75.0	1.4	4.4	3.5	2.5	10.1
10a″	−8.22	10.23	5	91.0	0.6	1.3	0.6	1.0	5.4
13a′	−8.56	10.57	6	73.5	6.9	3.1	11.0	0.5	3.4
12a′	−9.38	12.94	7	20.1	15.9	28.0	29.0		

15a′, 2.7% 2s (C4), 3.9% 5s (Rh); 11a″, 5.0% 2s (C4); 12a′, 2.4% 5p (Rh), 2.3% 5s (Rh)

orbital M = Ir	Xα energy (eV)	vertical IP(eV)	band assignt	% 5d Ir	% 2p C1	% 2p C2	% 2p C3	% 2p C4	% 2p O
16a′	−5.03	7.52	1	14.1	21.1	5.6	32.8	8.4	10.9
11a″	−6.44	9.85	4	18.6	0.2	45.8	15.2	4.1	1.8
15a′	−7.27	8.53	2	79.0		3.6	1.6	2.8	1.6
14a′	−7.95	9.49	3	68.2	2.1	5.7	4.8	2.6	12.1
10a″	−8.40	10.37	5	88.7	0.8	1.5	0.6	1.0	7.3
13a′	−8.73	10.84	6	71.0	7.2	3.5	11.2	0.5	4.8
12a′	−9.45	12.81	7	25.1	14.6	25.2	26.4		

15a′, 3.0% 2s (C4), 5.3% 6s (Ir); 11a″, 4.7% 2s (C4); 12a′, 2.3% 6p (Ir), 2.4% 6s (Ir)

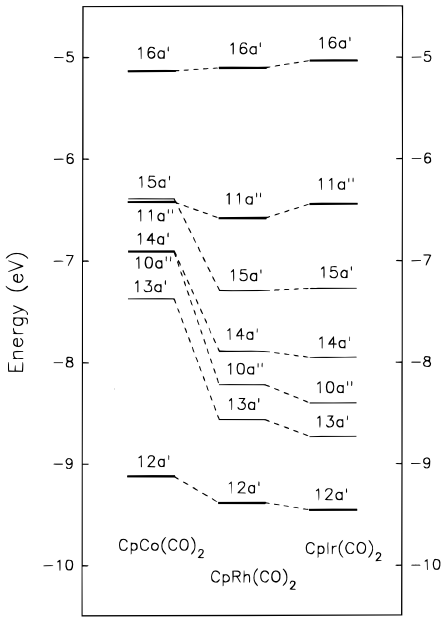

Figure 8. Xα-SW molecular orbital diagrams of $CpM(CO)_2$ molecules (M = Co, Rh, Ir). The thicker lines represent ligand-based MO's.

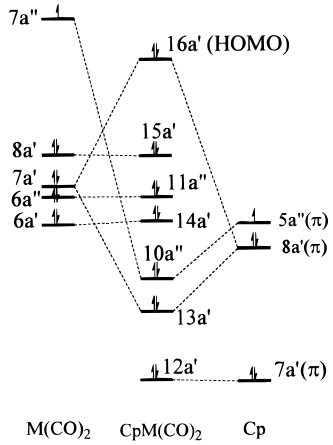

Figure 9. Fenske−Hall molecular orbital correlation diagram of $CpM(CO)_2$ from refs 4b and 21 (M = Co and Rh, orbitals are labeled in this paper).

A, and the shift of band B toward the high-binding-energy direction is more obvious in the Ir spectrum. The trend of binding energy for band B among the three compounds is 14.4 eV (Co) < 15.2 eV (Rh) ≈15.4 eV (Ir).

(b) Electronic Structures of $CpM(CO)_2$ (M = Co, Rh, and Ir) from Xα-SW Calculations. Xα-SW MO calculations were performed on $M(CO)_2$ radical fragments and the Cp radical. Our results are essentially the same as those reported earlier,[4b,19,20] and so they are not reported here.

The outer valence orbitals of $CpM(CO)_2$ are formed by combining $M(CO)_2$ and Cp radicals together. The calculated orbital compositions and Xα energy diagrams are shown in Table 1 and Figure 8. For comparison, the Fenske−Hall molecular orbital correlation diagram for $CpM(CO)_2$ (M = Co, Rh), reported in the literature,[4b,20] is plotted in Figure 9. In the present work, the

(19) (a) Mingos, D. M. P. In *Comprehensive Organometallic Chemistry*; Wilkinson, G., Ed.; Pergamon Press: Oxford, U.K., 1982; Vol. 3, pp 2−5. (b) Johnson, J. B.; Klemperer, W. G. *J. Am. Chem. Soc.* **1977**, *99*, 7132.

(20) Lichtenberger, D. L.; Blevins, C. H.; Ortega, R. B. *Organometallics* **1984**, *3*, 1614.

Table 2. Xα-SW Mainly MO Compositions and PES Band Assignments for $CpCo(CO)_2$ in Its Inner Valence Region (Predominating with σ Type Orbitals)

				Cp		CO				H	Co
orbital	Xα energy (eV)	vertical IP (eV)	band assignt	C % 2p	C % 2s	C % 2p	O % 2s	O % 2p	O % 2s	% 1s	% 3d
11a′	−10.93	14.40	A, B	85.8						13.3	
9a″	−10.99	14.40	A, B	83.7						14.7	
8a″	−11.64	14.40	A, B	65.2						25.3	
7a″	−12.25	14.40	A, B			22.1		73.9			
6a″	−12.41	14.40	A, B			24.1		74.3			
10a′	−12.41	14.40	A, B	41.0		9.5		29.5		18.4	
9a′	−12.56	14.40	A, B	35.0		12.0		33.5		15.6	
8a′	−12.60	14.40	A, B			25.9		69.8			
5a″ [a]	−13.25	14.40	A, B			27.9	26.3	5.4			29.4
7a′ [a]	−13.95	14.40	A, B			33.6	28.6	7.1			7.8
6a′	−15.78	17.64	C	52.8	7.8					37.8	
4a″	−16.03	17.64	C	29.6	34.3					35.8	
5a′	−16.03	17.64	C	34.8	27.3					37.2	
3a″	−17.63	18.36	D			4.2	11.1	56.0	28.5		
4a′	−17.65	18.36	D			3.3	12.6	54.9	28.8		
2a″	−19.34	20.03	E	12.3	64.5					22.1	
3a′	−19.87	20.03	E	13.5	68.2					17.2	
2a′	−23.25	22.77	F	10.6	82.0	4.7					
CO satellite		26.32	G								
CO satellite		29.89	H								
1a′	−35.47	35.04	I			21.4	17.8	18.3	42.4		
1a″	−35.47	35.04	I			21.5	17.8	18.3	42.4		

[a] Orbital 5a″ has 5.4% Co 4p, and orbital 7a′ has 5.5% Co 4p and 13.4% Co 4s.

The calculated electron configuration for the $CpCo(CO)_2$ molecule is

$$(\text{core})(12a')^2(13a')^2(10a'')^2(14a')^2(11a'')^2(15a')^2(16a')^2$$

and that for the Rh and Ir molecules is

$$(\text{core})(12a')^2(13a')^2(10a'')^2(14a')^2(15a')^2(11a'')^2(16a')^2$$

The following results are obtained for all three molecules from the C 2p compositional distribution on the Cp ring in Table 1: (1) the C 2p character distribution of 16a′ and 13a′ on the Cp ring is consistent with the schematic contour diagram of the Cp 8a′ orbital, indicating that they are the antibonding and bonding pair formed by interaction of one $M(CO)_2$ orbital in a′ symmetry with Cp 8a′; (2) the ring compositions of the 11a″ orbitals have the characteristic of Cp 5a″ distributions, showing that they are the bonding orbitals formed by interaction of 7a″ of $M(CO)_2$ with 5a″ of Cp; (3) for orbitals 12a′, the ring compositions show predominantly Cp 7a′ character.

The Xα molecular orbital energy diagrams of $CpM(CO)_2$ (Figure 8) show that the ordering for Co is in agreement with that calculated in the Fenske−Hall method (Figure 9), except that our bonding orbital from the combination of 7a″ of $Co(CO)_2$ and 5a″ of Cp is 11a″ rather than 10a″. Our orbital diagrams indicate that the ordering of 11a″ and 15a′ orbitals in Co is reversed in Rh and Ir molecules; whereas the Fenske−Hall calculations do not show this result.[4b,20] Of greater importance, the diagrams show that all the MO's with mainly metal d character (15a′, 14a′, 10a″, and 13a′) shift to more negative values in $CpRh(CO)_2$ and $CpIr(CO)_2$ molecules than in the $CpCo(CO)_2$ complex. However, the energies of three MO's with mostly ligand character (16a′, 11a″, and 12a′, mainly Cp character) remain relatively constant for the three complexes.

The Xα-SW MO compositions for $CpM(CO)_2$ in the inner valence region are listed in Tables 2−4. The MO's with predominant CO character are divided into four groups.

(1) *CO* 1π. They are the 7a″, 6a″, 9a′ and 8a′ orbitals, and all have compositions with more O than C 2p character, typical of CO 1π orbitals.

(2) CO 5σ with Considerable Metal d Composition. They are the 5a″ and 7a′ orbitals, and each has high C 2p and C 2s character, typical of sp hybridization in CO 5σ. Of importance, only these two MO's in the inner valence region have significant metal d character, supporting the assignment to a bonding orbital between metal and CO 5σ in the molecules. Moreover, the metal d compositional sequence for these two orbitals is Ir 5d (38.7% and 18.4%) > Rh 4d (37.1% and 16.1%) ≫ Co 3d (29.4% and 7.8%), indicating that the orbital mixing and degree of bonding between metal d and CO 5σ is 5d(Ir) > 4d(Rh) ≫ 3d(Co).

(3) CO 4σ. They are the 4a′ and 3a″ orbitals. These two orbitals show more oxygen 2p and 2s character than carbon 2p and 2s character, associated with the lone-pair electron orbital of oxygen with mainly sp-hybridized feature.

(4) CO 3σ. They are the 1a′ and 1a″ orbitals. Their characters suggest that their atomic origin is the sp-hybridized orbitals of carbon and oxygen.

Besides these four types of orbitals with CO character, all the other orbitals in the inner valence shell have predominant Cp character (Tables 2−4).

(c) Theoretical Calculations for Photoelectron Branching Ratios. We obtained theoretical cross sections using both the Gelius method[21] and the Xα method with Davenport's program[17] and then obtained branching ratios $BR_i = \sigma_i/\sum\sigma_i$, where σ_i is the calculated cross section to compare with the experimental BR_i values. In the Gelius treatment, the cross section of an

(21) (a) Gelius, U. In *Electron Spectroscopy*; Shirley, D. A., Ed.; North-Holland: Amsterdam, 1972; p 311. (b) Bancroft, G. M.; Malmquist, P.-Å.; Svensson, S.; Basilier, E.; Gelius, U.; Siegbahn, K. *Inorg. Chem.* **1978**, *17*, 1595.

Table 3. Xα-SW Mainly MO Compositions and PES Band Assignment for $CpRh(CO)_2$ in Its Inner Valence Region (Predominating with σ Type Orbitals)

				Cp		CO				H	Rh
orbital	Xα energy (eV)	vertical IP (eV)	band assignt	C % 2p	C % 2s	C % 2p	O % 2s	O % 2p	O % 2s	% 1s	% 4d
11a′	−11.26	14.09	A	85.6						13.4	
9a″	−11.31	14.09	A	83.1						14.9	
8a″	−11.88	14.09	A	67.0	5.0					25.3	
10a′	−12.83	14.09	A	63.5				3.6		28.5	
7a″	−13.06	14.09	A			23.7		75.7			
6a″	−13.20	14.09	A			24.9		72.9			
9a′	−13.26	14.09	A	4.1		23.8		67.2		2.0	
8a′	−13.40	14.09	A			26.3		68.9			
7a′ [a]	−13.82	15.18	B			31.0	30.6	5.0			16.1
5a″ [a]	−14.29	15.18	B			24.8	25.4	3.0			37.1
6a′	−16.12	17.66	C	55.3	4.9					37.9	
5a′	−16.30	17.66	C	32.4	30.4					36.7	
4a″	−16.36	17.66	C	29.8	34.2					35.6	
4a′	−18.42	18.44	D			4.0	9.7	55.3	30.8		
3a″	−18.43	18.44	D			4.2	9.4	55.6	30.7		
2a″	−19.63	20.55	E	12.4	64.4					21.7	
3a′	−20.21	20.55	E	13.6	68.1					17.1	
2a′	−23.50	22.78	F	10.6	82.3					4.7	
CO satellite		26.25	G								
CO satellite		29.59	H								
2a′	−37.66	35.17	I			22.6	17.9	20.1	39.3		
1a″	−37.66	35.17	I			22.6	18.0	20.1	39.3		

[a] Orbital 5a″ has 3.4% Rh 5p, and orbital 7a′ has 4.1% Rh 5p and 8.9% Rh 5s.

Table 4. Xα-SW Mainly MO Compositions and PES Band Assignments for $CpIr(CO)_2$ in Its Inner Valence Region (Predominating with σ Type Orbitals)

				Cp		CO				H	Ir
orbital	Xα energy (eV)	vertical IP (eV)	band assignt	C % 2p	C % 2s	C % 2p	O % 2s	O % 2p	O % 2s	% 1s	% 5d
11a′	−11.18	14.09	A	85.6						13.3	
9a″	−11.23	14.09	A	83.2						14.7	
8a″	−11.81	14.09	A	67.3	4.6					25.7	
10a′	−12.76	14.09	A	60.4				7.1		27.2	
7a″	−12.92	14.09	A			23.7		75.9			
6a″	−13.09	14.09	A			25.2		71.4			
9a′	−13.26	14.09	A	8.3		22.3		60.7		4.1	
8a′	−13.28	14.09	A			26.6		67.5			
7a′ [a]	−14.30	15.42	B			29.1	28.0	4.2			18.4
5a″ [a]	−15.07	15.42	B			24.4	23.8	3.1			38.7
6a′	−16.08	17.71	C	55.4	3.9					37.8	
5a′	−16.23	17.71	C	31.1	31.4					36.6	
4a″	−16.30	17.71	C	29.5	34.2					35.7	
4a′	−18.27	18.66	D			3.8	10.2	55.2	30.6		
3a″	−18.27	18.66	D			3.9	10.0	55.4	30.5		
2a″	−19.57	20.77	E	12.2	64.0					21.5	
3a′	−20.16	20.77	E	13.4	68.0					17.1	
2a′	−23.43	22.91	F	10.5	81.9					4.7	
CO satellite		26.37	G								
CO satellite		30.25	H								
1a′	−37.29	34.34	I			22.3	17.8	19.9	39.9		
1a″	−37.30	34.34	I			22.4	17.8	19.9	39.9		

[a] Orbital 5a″ has 4.0% Ir 6p, and orbital 7a′ has 4.8% Ir 6p and 9.7% Ir 6s.

individual MO is assumed to be proportional to the sum of the atomic cross sections (σ_{A_j}) of its components weighted by the "probability" $(P_{A_j})_i$ of finding the *i*th molecular orbital an electron belonging to the atomic orbital A_j:

$$\sigma_i \propto \sum_j (P_{A_j})_i \sigma_{A_j} \qquad (1)$$

where $(P_{A_j})_i$ is given approximately by the orbital composition from our Xα calculations, and σ_{A_j} values are the theoretical atomic cross sections as a function of photon energy. In this work, Yeh and Lindau's data,[22] obtained by the Hartree−Slater central field method, were used. A qualitative guide to the variations in molecular cross sections and branching ratios can be obtained by looking at the important atomic cross sections in Figure 10. Thus, all metal d orbitals show a large increase in cross section above threshold, before decreasing in markedly different ways at higher energies. In contrast, the C 2p and O 2p orbitals show a monotonic decrease in cross section over the whole

(22) Yeh, J. J.; Lindau, I. *At. Nucl. Data Tables* **1985**, *32*, 1.

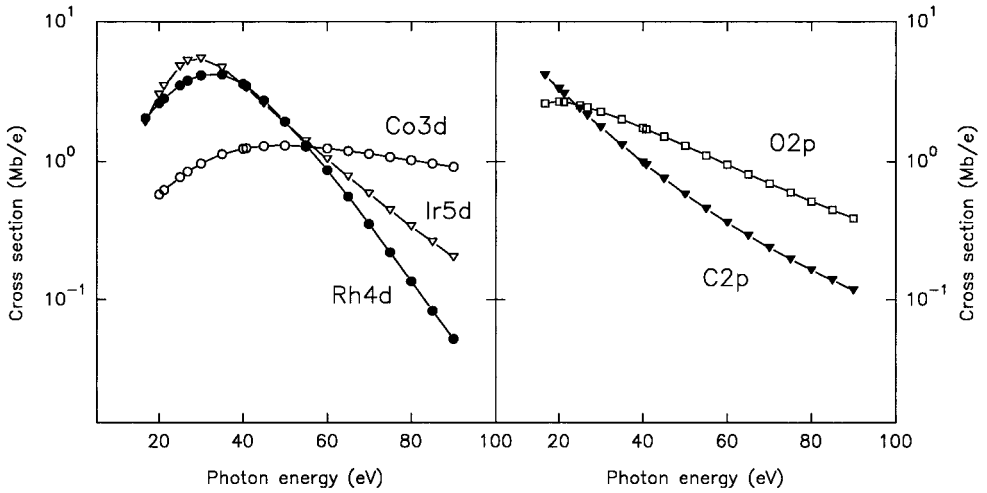

Figure 10. Photoionization cross sections for atomic Co 3d, Rh 4d, Ir 5d, C 2p, and O 2p subshells.[22]

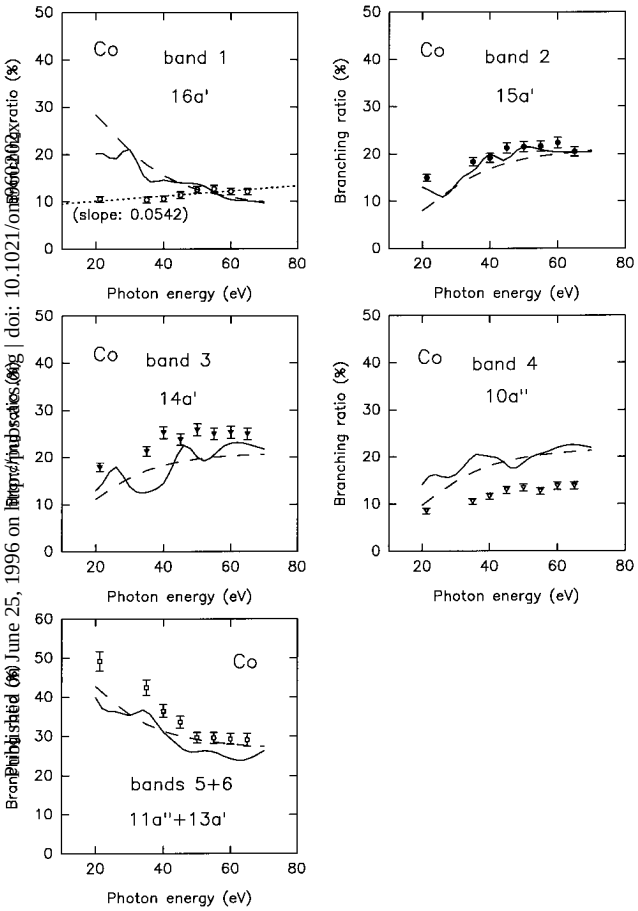

Figure 11. Comparison of experimental branching ratios (symbols) with Xα ones (solid line) and ones from the Gelius model (dashed line) for the valence bands 1−6 of CpCo(CO)$_2$ in the photon energy range 21.2−70 eV. Our band assignments are indicated on each plot. The slope of the first-order regression line (dotted line) for the experimental BR's of band 1 is indicated.

range. This behavior gives rise to the changes in the ratio of the M *n*d/C2p cross sections, which are reflected in the branching ratio changes.

The theoretical branching ratios for MO's in the outer valence region of CpCo(CO)$_2$ are plotted in Figure 11 (solid line, from the Xα calculation; dashed line, by the Gelius model treatment). They demonstrate that the general trends of branching ratios of the three metal d based MO's (15a′, 14a′, and 10a″) increase from 21.2 to 70 eV, and the curves containing the two mainly ligand

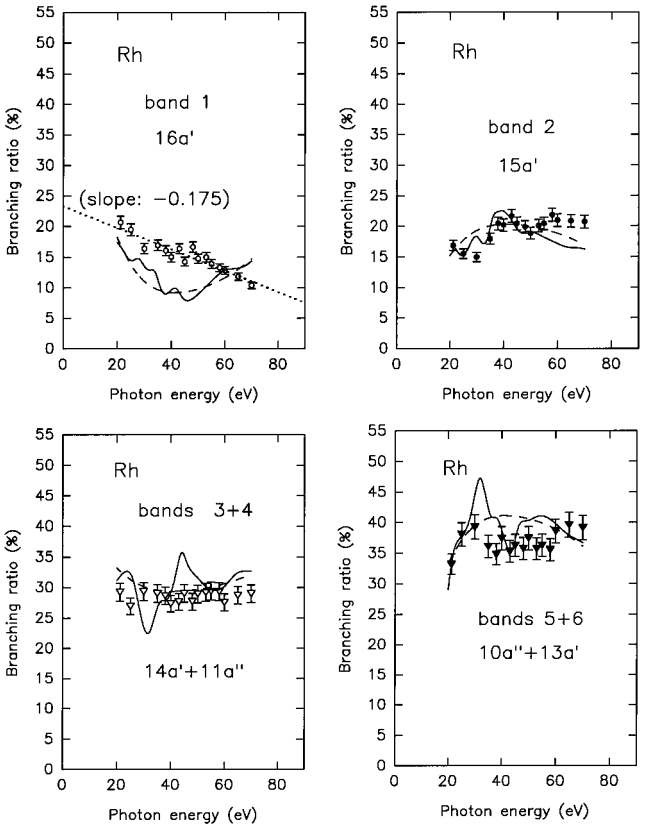

Figure 12. Comparison of experimental branching ratios (symbols) with Xα ones (solid line) and ones from the Gelius model (dashed line) for the valence bands 1−6 of CpRh(CO)$_2$ in the photon energy range 21.2−70 eV. Our band assignments are indicated on each plot. The slope of the first-order regression line (dotted line) for the experimental BR's of band 1 is indicated.

MO's (16a′ and 11a″) show a decrease in branching ratio from low to high photon energy. This decrease of branching ratio for ligand-based MO's is also displayed for the 16a′ orbitals for Rh and Ir analogues from 21.2 to 45 eV (Figures 12 and 13). Since the metal 4d and 5d orbital cross sections decrease rapidly to a Cooper minimum[23] at high photon energy, the theoretical branching ratios of these two ligand-based MO's increase when the photon energy is higher than 45 eV. For the theoretical branching ratios of the metal d based

(23) Berkowitz, J. *Photoabsorption, Photoionization, and Photoelectron Spectroscopy*; Academic Press: New York, 1979; pp 35−72.

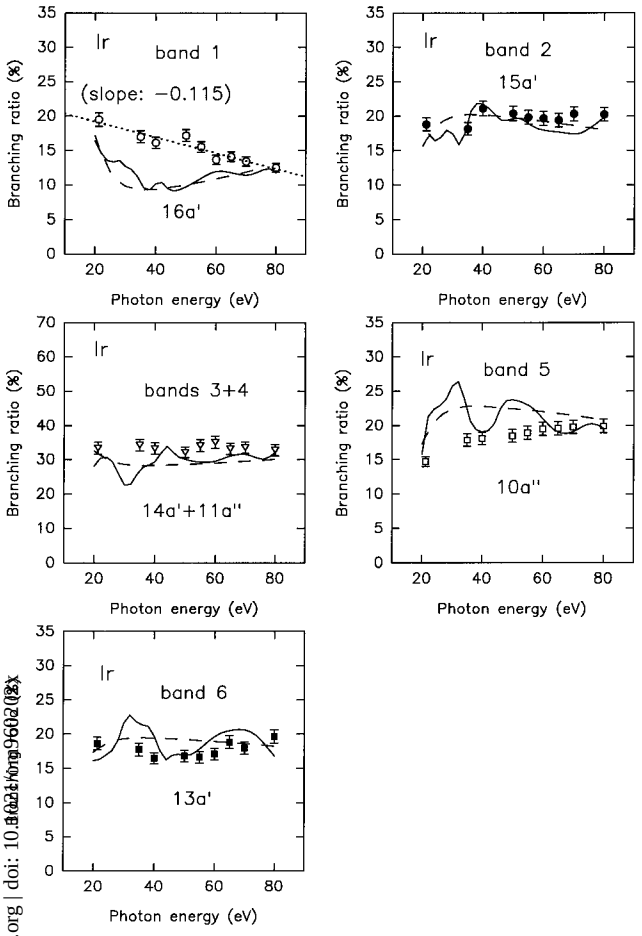

Figure 13. Comparison of experimental branching ratios (symbols) with Xα ones (solid line) and ones from the Gelius model (dashed line) for the valence bands 1−6 of $CpIr(CO)_2$ in the photon energy range 21.2−70 eV. Our band assignments are indicated on each plot. The slope of the first-order regression line (dotted line) for the experimental BR's of band 1 is indicated.

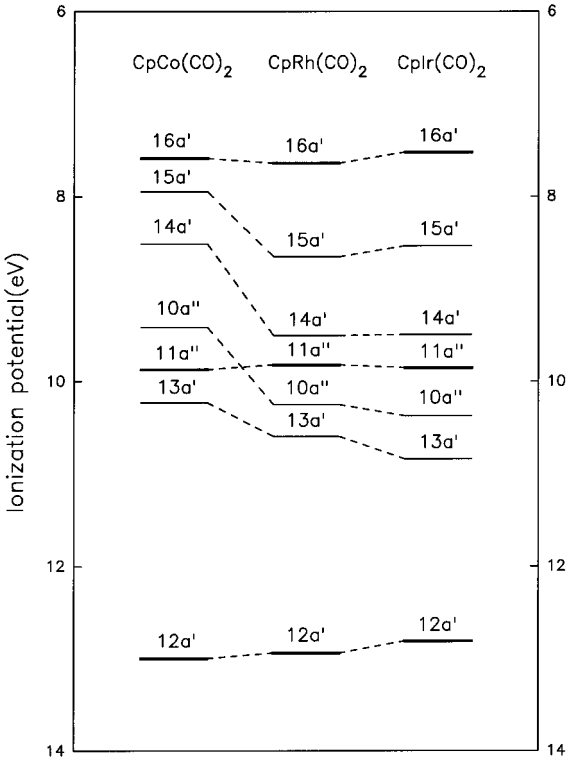

Figure 14. Ionization potential (IP) diagrams of $CpM(CO)_2$ (M = Co, Rh, Ir) assigned by using variable-energy photoelectron spectroscopy in this work. The thicker lines represent those ligand-based MO's.

MO's (15a′) for Rh and Ir, we can also see the influence of the Cooper minimum, *i.e.*, beyond 40 eV the branching ratios decrease (for Rh) or go flat (for Ir) rather than increase as in the low-photon-energy region.

Discussion

The MO calculations (see Table 2) all give seven MO's in the outer valence region for the three compounds. The Ir spectrum gives exactly seven photoelectron bands (Figure 2), whereas the Rh and Co spectra have many closely overlapping bands (especially for $CpCo(CO)_2$). The whole or partial overlapping of bands makes MO assignments based on any analysis of relative band intensity difficult for all three compounds. Our challenge is to match the observed and theoretical branching ratios. Our assignments for outer and inner valence spectra based on all available information (*e.g.* the matching between observed and theoretical branching ratios, the intensity difference between two helium-light photon energies, band width, band shift, reported work on pure ligand spectra of the inner shell, and calculated energy values) are given in Tables 1−4 and Figure 14.

(a) Assignment for $CpCo(CO)_2$. Experimental branching ratios (BR) of bands for $CpCo(CO)_2$ are plotted in Figure 11. They show that the BR's for bands 2−4 are similar and increase from low to high photon energy. These bands must be assigned to the three orbitals (15a′, 14a′, and 10a″) of high Co 3d character (Table 1). The BR of bands 5 + 6 is large but decreases rapidly: these bands are assigned to the orbitals 11a″ (with mainly ligand character) and 13a′. The BR for band 1 is similar to that of band 4 but increases even more slowly: this band must be assigned to a MO with intermediate metal d and ligand character (16a′). The theoretical branching ratios from Xα cross-section calculation and Gelius model treatment for each MO are plotted in Figure 11 to get the closest match between them and the experiment (BR's for 11a″ and 13a′ are combined in one curve for each calculation to match the experimental results for bands 5 + 6). It is shown that the best matches between theory and experiment are observed for bands 2, 3, and 5 + 6. For band 4, the absolute BR values deviate from the theoretical values, perhaps because its overlapping neighbor, bands 5 + 6, makes the fitting less reliable. However, the trends of experimental and theoretical BR's for band 4 are generally in agreement. The trends of experimental and theoretical BR's for the first band do not agree very well. The theoretical trend shows that this band, like band 5 + 6, decreases in intensity from low to high photon energy, while the experiment result shows that it is more like bands 2−4, due to metal d based MO's, with intensity increasing over the whole photon energy region. This suggests that *the actual metal d character of band 1 is even larger than that calculated by Xα-SW.* On the basis of the band intensity variation between He I and 60 eV photon energy, we assign band 7 (Figure 4) to 12a′, a mainly ligand Cp (7a′) orbital. The IP sequence from the MO assignments (Figure 14) is 12a′ > 13a′,11a″ > 10a″ > 14a′ > 15a′ > 16a′, which can be compared to the theoretical MO sequence in the ground-

state electronic configuration (Figure 8), which is (core)-$(12a')^2(13a')^2(10a'')^2(14a')^2(11a'')^2(15a')^2(16a')^2$. We note that the IP sequence is not the same as that derived from Koopmans' theorem, *i.e.*, the MO's with large metal d character systematically move to lower IP than predicted by Koopmans' theorem.

The MO assignment made by us for the IP ordering is the same as that reported previously.[4b] The intensity of the first band does not decrease relative to bands 2 and 3 as described previously[4b] but has intensity similar to those of bands 2 and 3 over the whole photon energy range. This observation is consistent with previous work on CpCo(diene),[4a] which also shows little intensity change in the low-IP region from He I to He II.

(b) Assignments for $CpRh(CO)_2$ and $CpIr(CO)_2$. Experimental branching ratios of bands for $CpRh(CO)_2$ and $CpIr(CO)_2$ are plotted in Figures 12 and 13. Bands 3−6 in Rh spectra and bands 3 and 4 in Ir spectra largely overlap, making the determination of experimental branching ratios unreliable for individual bands. Thus, some unresolved bands are combined to plot the branching ratios.

For both of these compounds, the first band is well resolved. On the basis of the matching between experimental and theoretical branching ratios, we assign it to 16a′, a ligand-based MO in each complex. In each case, the experimental BR decreases from low to high photon energy, strongly indicating that this MO has mostly ligand character. This contrasts sharply with the trend in experimental BR variation for the first band of $CpCo(CO)_2$, which is roughly constant over the whole photon energy range, indicating considerable metal d character. The theoretical branching ratios of HOMO's (16a′) for $CpRh(CO)_2$ and $CpIr(CO)_2$ are in rough agreement with experiment, except that the theoretical curves have a minimum between 40 and 50 eV photon energy; this is due to the sharp decrease in *n*d cross sections at about 40 eV (Figure 10).

The 15a′ MO's are assigned to the second bands in the Rh and Ir spectra. The experimental BR increases for the Rh spectra and shows little change for the Ir spectra. This shows the difference in metal d character associated with them (84% Rh 4d and 79% Ir 5d, Table 2), indicating enhanced metal−ligand interaction in the third-row transition-metal compounds. This is shown in Table 1, in which all valence MO's in $CpIr(CO)_2$ have less metal d character than the corresponding MO's in $CpRh(CO)_2$, indicating stronger mixing between metal and ligand orbitals in the Ir compound. The enhanced metal-ligand orbital mixing in the third-row transition-metal compound makes the contrast in band intensity variations between metal d and ligand-based MO's in Ir spectra less striking than in the Rh spectra (Figures 6 and 7).

Bands 3 and 4 in the Rh and Ir spectra can be assigned by considering these two compounds together. The BR's of bands 3 and 4 are not separated for either compound. The assignments are made by considering the general matching of the sums of BR's between theory and experiment (Figures 12 and 13), by comparing the He I and He II band intensities (for Rh, Figure 5), and by checking the difference of band intensities between He I and variable-energy PE spectra (for Ir, Figures 2 and 7). All these data support the assignment of band 3 to 14a′, a MO with relatively large metal d character (75.0% Rh 4d, 68.2% Ir 5d), and the assignment of band 4 to 11a″, a MO with small metal d and large ligand character (23.9% Rh 4d, 18.6% Ir 5d).

Although the BR's for bands 5 and 6 are not separated for Rh (Figure 12), they can be separated for Ir (Figure 13). The theoretical and experimental BR's in Figures 12 and 13 suggest the assignment of band 5 to 10a″, a metal d based MO (91.0% Rh 4d, 88.7% Ir 5d) and the assignment of band 6 to 13a′, a MO with less metal d character (73.5% Rh 4d, 71.0% Ir 5d). The difference in metal d characters is clearer for the Ir compound (Figure 13), which shows that the BR of band 5 increases, and that of band 6 is relatively constant from low to high photon energy.

On the basis of the band intensity variations between He I and 60 eV photon energy, we assign band 7 (Figure 4) of these two compounds to 12a′, a mainly ligand Cp (7a′) orbital (Figure 9).

The IP sequence from the MO assignments (Figure 14) for these two compounds is 12a′ > 13a′ > 10a″ > 11a″ > 14a′ > 15a′ > 16a′. By comparison with the MO sequence in the ground-state electronic configurations for $CpM(CO)_2$ (M = Rh, Ir; Figure 8), which is (core)-$(12a')^2(13a')^2(10a'')^2(14a')^2(15a')^2(11a'')^2(16a')^2$, it can be also seen that the IP sequence is not the same as that derived from the Xα calculations and Koopmans' theorem. In particular, the MO's with large metal d character systematically shift to IP lower than that predicted by Koopmans' theorem.

(c) Evaluation of Ground-State d Energy Difference (ΔE) in the Transition-Metal Group and Correlation between ΔE and ΔIP for MO's in the Outer Valence Region. The trends in our experimental branching ratios for the three compounds show two distinct features: (1) for the cobalt spectra, the BR values of bands 5 + 6 decrease sharply from low to high photon energy, while BR's for other bands increase slightly over the whole photon energy region; (2) for rhodium and iridium spectra, the BR's of the first bands decrease from low to high photon energy and those for others are constant or increase over the photon energy region. These features generally demonstrate that the MO's with mainly metal d character for the cobalt spectra are located more in the low-IP region, while those in the rhodium and iridium spectra are located more in the high-IP region.

The cause for this IP difference (ΔIP) between energies of the metal d orbitals for the first- and second-third-row transition metals has not been clearly elucidated. The effect is larger for late-transition-metal than for early-transition-metal compounds.[3a] There are two theories to rationalize the trends in binding energies. One theory suggests that the energy difference is a ground-state effect,[3a,4a,] and the other that it is a difference in the ionized state,[4b,24] *i.e.* a large difference in reorganization energy (=electron relaxation plus correlation energies) on descending a late-transition-metal group. The result from our study gives strong evidence to support the ground-state rationalization. The advantage of using the variable-energy photoelectron technique is that it can not only help us to assign the IP orderings but can also show the variations in the

(24) (a) Calabro, D. C.; Lichtenberger, D. L. *Inorg. Chem.* **1980**, *19*, 1732. (b) Lichtenberger, D. L.; Kellogg, G. E. *Acc. Chem. Res.* **1984**, *3*, 1623.

(25) (a) Higginson, B. R.; Lloyd, D. R.; Connor, J. A.; Hillier, I. H. *J. Chem. Soc., Faraday Trans. 2* **1974**, *70*, 1418. (b) Cowley, A. H. *Prog. Inorg. Chem.* **1979**, *26*, 46.

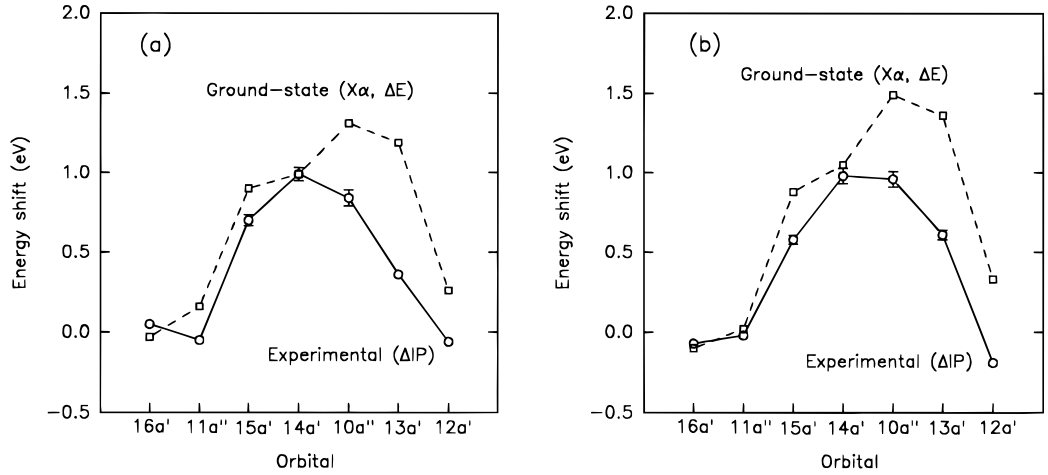

Figure 15. Correlation of ground-state energy difference (ΔE) with experimental IP difference (ΔIP): (a) between $CpRh(CO)_2$ and $CpCo(CO)_2$; (b) between $CpIr(CO)_2$ and $CpCo(CO)_2$. $\Delta E_i = -[E_i(\text{Rh or Ir}) - E_i(\text{Co})]$. $\Delta IP_i = IP_i(\text{Rh or Ir}) - IP_i(\text{Co})$. Ligand-based MO's (metal d <32%): 16a′, 11a″, and 12a′. Metal d based MO's (metal d >68%): 15a′, 14a′, 10a″, and 13a′.

ion state orbital compositions for corresponding MO's among a group of analogues. This information is important, supporting the ground-state energy difference down a late-transition-metal group. In particular, in molecules $CpM(CO)_2$ (M = Co, Rh, Ir) which have C_s symmetry, no totally nonbonding metal or ligand MO's exist, but all MO's in the outer valence region show some bonding between metal d and ligand orbitals (Table 1). Hence, they provide us with suitable molecules to investigate the difference of orbital compositions in a group. This series is much more useful for this purpose than the series $M(\eta^3\text{-}C_3H_5)_2$ (M = Ni, Pd, Pt),[3a] since symmetry ensures the presence of nonbonding MO's for the $M(\eta^3\text{-}C_3H_5)_2$ series and since the nonbonding MO's in $M(\eta^3\text{-}C_3H_5)_2$ strongly overlap with other bands.

Both the variable-energy photoelectron spectroscopy and Xα-SW calculations on $CpM(CO)_2$ indicate that the ΔIP for the late-transition-metal complexes results from the ground-state difference (ΔE, *i.e.* 3d (Co) > 4d (Rh) ≈ 5d (Ir)). This conclusion is supported by the following analyses.

(1) Difference in Slopes among Experimental Branching Ratio Curves for the HOMO's of the Three Compounds. In Figures 11−13, the slopes of the linear regressions of experimental branching ratios of the HOMO's (16a′) are strikingly different between Co and Rh or Ir compounds. They show that the curve for the $CpCo(CO)_2$ HOMO is relatively flat (slope 0.0542), indicating its small amount of ligand character, while those for $CpRh(CO)_2$ and CpIr(CO) HOMO's incline apparently negatively (slope −0.175 and −0.115, respectively), showing their greater ligand character. This difference in slopes among experimental branching ratio curves for the HOMO's of the three compounds (Figures 11−13) correctly reflects the experimental facts that the relative intensity of band 1 of the Co compound steadily increases *along with the other Co 3d based bands* (bands 2−4; Figure 3) and that the intensities of bands 1 for the Rh and Ir compounds decrease relative to the other bands as the photon energy increases (Figures 6 and 7). Thus, one conclusion immediately arises from this experimental branching ratio analysis: the metal d orbital compositions among the HOMO's of the three compounds *must* be very different. From the composition analyses we know that the 16a′ MO in all the three compounds originates from the antibonding combination of $M(CO)_2$ 7a′ with Cp 8a′ (Table 1). Thus, the change of ligand composition in this orbital from Co to Rh or Ir reflects the change of atomic metal d energies in the ground state. The smaller ligand character of the Co HOMO's than those of Rh or Ir HOMO's revealed in this work yields the ground-state d energy sequence in the atomic case: 3d (Co) > 4d (Rh) ≈ 5d (Ir). This trend is consistent with our calculated metal d compositions for HOMO's among the three compounds (Table 1): Co 3d (24.9%) > Rh 4d (16.0%) ≈ Ir 5d (14.1%). The Co 3d composition shown from the experimental BR is even higher than 24.9%, as discussed earlier.

(2) Correlation between ΔE and ΔIP for MO's in the Outer Valence Region. The ground-state molecular orbital energy diagrams from Xα-SW calculations and IP orderings of these MO's assigned by our variable-energy photoelectron spectroscopy for the three compounds are plotted in Figures 8 and 14, respectively. A common trend derived from the ground-state MO sequences and the IP orderings is that all those MO's with mainly metal 4d (Rh) and 5d (Ir) characters shift downward in the diagrams relative to the MO's with mainly 3d (Co) character, while the ligand-based MO's remain relatively constant when the Co metal in $CpM(CO)_2$ is replaced with Rh or Ir. These correlations in ground-state energy differences (ΔE) and IP difference (ΔIP) are clearly seen in Figure 15, which suggest that the cause of the IP shift is mainly from the ground-state energy shift of these MO's, which reflects the atomic d energy sequence 3d (Co) > 4d (Rh) ≈ 5d (Ir). Obviously, the correlation suggests strongly that the differential reorganization energies are not as large as previously thought.[4b,24]

We have shown that in late transition metals (this work and ref 3) the metal d IP's increase greatly from the first to the second row. What is the periodic trend in this metal d IP difference? Table 5 lists typical metal *n*d ionizations reported for some organometallic compounds. These data show that, for the early-transition-metal compounds, the IP difference (ΔIP) between rows is not large (only 0.1 eV between $Mo(CO)_6$ and $Cr(CO)_6$). However, the difference between the second and first row increases for the late-transition-metal complexes (1.17 and 1.9 eV for the Ni and Cu groups respectively; Figure 16). The differences between the third row and second row are small over the whole period. For the

Table 5. Reported Ionization Potentials (eV) of Mainly Metal d MO's for Typical Organometallic Compounds and Difference of Ionization Potentials (ΔIP) betweeen Second- and First-Row-Metal Organometallic Compounds

compd	assignt	M (1st row)	M (2nd row)	M (3rd row)	ΔIP	ref
$M(CO)_6$	t_{2g}	Cr, 8.40	Mo, 8.50	W, 8.56	0.10	25
$CpM(CO)_3$[a]	e	Mn, 8.05		Re, 8.39	0.34	28
$M(\eta^5\text{-}C_5H_5)_2$[b]	e_{2g}	Fe, 6.86	Ru, 7.45		0.59	29, 25b
$CpM(CO)_2$	a′	Co(15a′), 7.94	Rh(15a′), 8.65	Ir(15a′), 8.53	0.71	this work
$M(\eta^3\text{-}C_3H_5)_2$	a_g	Ni(13ag), 7.64	Pd(17ag), 8.81	Pt(21ag), 8.64	1.17	3a
$(hfac)MP(CH_3)_3$[c]	a′	Cu(12a′), 9.77	Ag(10a′), 11.7		1.9	3c

[a] For the Mn group, the ΔIP is calculated between the Re and Mn compounds. Spin−orbit splitting has been resolved for the $CpRe(CO)_3$ e(5d) band, so the IP value for it is the average of the two spin−orbit splitting members. [b] Another group of useful data are the $e_{2g}(nd)$ IP values for $M(\eta^5\text{-}MeC_5H_4)2$:[29b] Fe, 6.72 eV; Ru, 7.25 eV; Os, 7.24 ref 30 for the $Re(\eta^5\text{-}C_5H_5)_2$ analogue. [c] hfac = $CF_3C(O)CHC(O)CF_3$.

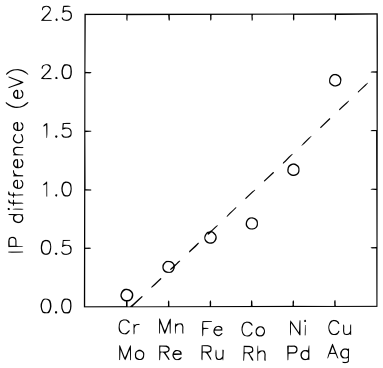

Figure 16. Observed difference of ionization potentials between second- and first-row transition-metal complexes for the "HOMO" metal d orbitals.

late-transition-metal organometallic compounds, theoretical calculations in this work and others[3a,c] have shown that the trend in d energy difference in the *ground* state is consistent with the observed IP difference. For example, for the early-transition-metal complexes, Arratia-Perez and Yang[26] have used the self-consistent-field−Xα−Dirac-scattered-wave (SCF-Xα-DSW) molecular orbital method to calculate the bonding in $M(CO)_6$ (M = Cr, Mo, W). Their calculated eigenvalues for the $t_{2g}(nd)$ orbitals are $Cr(CO)_6$ (−7.317, −7.352 eV), $Mo(CO)_6$ (−7.212, −7.288 eV), and $W(CO)_6$ (−7.446, −7.675 eV). Also, the experimental trend in ground-state d energies over the early- and late-transition-metal region shown in Table 5 and Figure 16 is in agreement with Ziegler's calculations.[3a,27] These results strongly support our assertion that the trend in IP's is dominated by the trend in ground-state energies and not differences in relaxation energies between the first- and second-row transition elements.

(d) Inner Valence Spectra. The broad-range high-resolution photoelectron spectra of the three complexes are shown in Figure 4. These complete valence and inner valence spectra, and those of other organometallics,[3a,c,6,18] are the first to be published for *organometallic* molecules. All the valence bands are readily seen in these spectra. In addition, the broad inner valence bands are also evident. These high-quality spectra, taken in less than 15 min, demonstrate the power of our photoelectron spectrometer combined with monochromatized synchrotron radiation.

The theoretical MO energies and orbital compositions for $CpM(CO)_2$ (M = Co, Rh, Ir) from our ground-state Xα-SW calculations are listed in Tables 2−4, along with our experimental photoelectron energies and assignments. One striking difference in the inner valence spectra between $CpM(CO)_2$ (M = Co, Rh, Ir) and $M(\eta^3\text{-}C_3H_5)_2$ (M = Ni, Pd, Pt)[3a] is that, in $M(\eta^3\text{-}C_3H_5)_2$, the inner valence spectra (beyond 12.6 eV) are almost identical for M = Ni, Pd, Pt. In contrast, for $CpM(CO)_2$ complexes large differences appear among the three compounds around 14.40 eV binding energyl *i.e.* bands A and B overlap in the Co spectrum (14.40 eV), but these bands are resolved in the Rh (14.09, 15.18 eV) and Ir (14.09, 15.42 eV) spectra. This separation of band B from band A in the Rh and Ir spectra is primarily due to the shift of band B to higher binding energy in Rh and Ir spectra compared to the Co spectrum. Based on two factors, we assign band B in the spectra of $CpCo(CO)_2$, $CpRh(CO)_2$ and $CpIr(CO)_2$ to the MO's 7a′ and 5a″. First, the intensity change between He I (Figure 2 in ref 4b) and 60 eV photon energy indicates a high metal d character, and only these two MO's bear high metal d characters (7.8% and 29.4% Co 3d, 16.1% and 37.1% Rh 4d, and 18.4% and 38.7% Ir 5d; see Tables 2−4). Second, the shifts of energies of these MO's between Co and Rh or Ir compounds are the greatest for the 5a″ orbitals. The absolute energy difference of all other MO's between $CpCo(CO)_2$ and the other two analogues are less than 0.81 eV. The 5a″ MO's have a 1.04 eV difference between Rh and Co and 1.82 eV difference between Ir and Co (in both cases, the 5a″ MO in the heavier metal compounds has a more negative value than in the Co compound), corresponding to an observed 0.78 eV shift of band B from Co to Rh and 1.02 eV from Co to Ir. These shifts are again consistent with the ground-state d energy sequence 3d (Co) > 4d (Rh) ≈ 5d (Ir), derived in the outer valence studies.

All other bands in the inner valence spectra of $CpM(CO)_2$ show little difference when M = Co, Rh, Ir, and so the same assignments can be made for the three compounds. The CO 1π based orbitals (7a″, 6a″, 9a′, and 8a′) are assigned to bands A, which are overlapped with four Cp-based orbitals (11a′, 9a″, 8a″, and 10a′) with mainly C 2p and H 1s characters. Another group of Cp-based orbitals (6a′, 5a′, and 4a″) are assigned to bands C. The CO 4σ orbitals (3a″ and 4a″) are assigned to bands D. Bands E and F are assigned to the remaining two groups of Cp-based orbitals (2a″ and 3a′, and 2a′), respectively. Bands G and H are assigned to the CO satellites which have been defined in the literature.[31] The last two orbitals (1a′ and 1a″), with mainly CO 3σ characters, are assigned to bands I. The

(26) Arratia-Perez, R.; Yang, C. Y. *J. Chem. Phys.* **1985**, *83*, 4005.
(27) Ziegler, T.; Tschinke, V.; Ursenbach, C. *J. Am. Chem. Soc.* **1987**, *109*, 4825.
(28) Calabro, D. C.; Hubbard, J. L.; Blevins, C. H., II; Andrew, C. C.; Lichtenberger, D. L. *J. Am. Chem. Soc.* **1981**, *103*, 6839.
(29) (a) $Fe(\eta^5\text{-}C_5H_5)_2$: Rabalais, J. W.; Werme, L. O.; Bergmark, T.; Karlsson, L.; Hussain, M.; Siegbahn, K. *J. Chem. Phys.* **1972**, *57*, 1185. (b) $Ru(\eta^5\text{-}C_5H_5)_2$: Evans, S.; Green, M. L. H.; Jewitt, B.; Orchard, A. F.; Pygall, C. F. *J. Chem. Soc., Faraday Trans. 2* **1972**, *68*, 1847.
(30) Cooper, G.; Green, J. C.; Payne, M. P. *Mol. Phys.* **1988**, *63*, 1031.
(31) Nilsson, A.; Mårtensson, N.; Svensson, S.; Karlsson, L.; Nordfors, D.; Gelius, U.; Ågren, H. *J. Chem. Phys.* **1992**, *96*, 8770.

above assignments for CO orbitals are basically consistent with those published for inner valence photoelectron spectra of free carbon monoxide[9,32] (by using synchrotron radiation) and that of $Cr(CO)_6$ (by using a traditional Al Kα light source).[31] Note that in each group of orbitals for the three compounds, the orbital characters are basically similar among the individual orbitals, and their orbital eigenvalues are also close. The vertical ionization potential for each band and the absolute average eigenvalue of the correspondent orbital group are roughly correlated except for bands A, which are very broad, and bands I, whose vertical IP's are less reliable since they are so weak and broad.

(e) Correlation of ΔE with the Group Trends in Bonding between Metal d and CO Orbitals. The results of our Xα-SW calculations have shown that (1) the degree of bonding between metal and CO $2\pi^*$ (CO back-bonding) is 3d(Co) > 4d(Rh) > 5d(Ir) (trend I), (2) the degree of bonding between metal and CO 5σ is Ir > Rh > Co (trend II), (3) the degree of bonding between metal d and CO 1π is 5d(Ir) > 4d(Rh) > 3d(Co) (trend III). How are these trends correlated with the ground-state d energy difference (ΔE) between the first and second or third row of late transition metals? The logical answer is that the energies of the 3d orbitals of the cobalt atom are closer to that of the CO $2\pi^*$ orbital than those of 4d(Rh) and 5d(Ir). Thus the degree of CO $2\pi^*$ back-bonding in the Co compound is the highest among the group (trend I). On the other hand, the energies of 4d(Rh) and 5d(Ir) are closer to those of CO 5σ and 1π than that of 3d(Co); therefore, the degrees of bonding between metal d and CO 5σ and 1π in the Rh and Ir compounds are larger than those in the Co compounds (trends II and III).

(32) (a) Krummacher, S.; Schmidt, V.; Wuilleumier, F.; Bizau, J. M.; Ederer, D. *J. Phys. B: At. Mol. Phys.* **1983**, *16*, 1733. (b) Liu, Z. F.; Bancroft, G. M.; Coatsworth, L. L.; Tan, K. H. *Chem. Phys. Lett.* **1993**, *203*, 337.

Conclusions

Variable-energy outer valence and inner valence photoelectron spectra of the $CpM(CO)_2$ complexes (M = Co, Rh, Ir) have been recorded between 21.2 and 70 eV photon energies. The spectra have been assigned using both ground-state Xα-SW calculations combined with a comparison of the experimental and theoretical branching ratios. The spectrum of the Co complex differs considerably from the spectra of the Rh and Ir complexes. The calculated MO energies and the experimental IP's, along with the calculated and observed branching ratios, all indicate that these large changes in spectra are due to the ground-state d orbital energies decreasing in the order 3d > 4d ≈ 5d. These changes for this group of compounds are consistent with other experimental and theoretical analyses across and down the transition-metal series.

Acknowledgment. We are very grateful for the financial support of the NSERC (Canada), for the continued assistance from the staff at the Aladdin Synchrotron, and other assistance from Mrs. J. Z. Xiong, Drs. J. S. Tse and Z. F. Liu, and Mr. Z. F. Yin. We also acknowledge the support of NSR Grant No. DMR-9212658 to the Synchrotron Radiation Centre.

OM960202X